NUMERICAL ANALYSIS OF SPALLATION FAILURE OF THIN PLATES UNDER SHOCK DEFORMATION

I. A. Volkov

UDC 539.375

It is well known [1] that upon reflection of a compression pulse from a free surface or contact boundary with a material of lower acoustic rigidity, tensile stresses develop within a body which under certain conditions can lead to its failure by spallation. Dissatisfaction with the results of a static approach to the problem of spallation failure has led on the one hand, to a search for new failure criteria, and on the other, to study of spallation at the microlevel, with development of a quantitative description of degradations and clarification of the role of material microstructure in destructive processes [2]. In recent years an approach has been developed to describe spallation failure, in which certain key variables are introduced into the defining relations (equations of state) with corresponding kinetic expressions which characterize formation of microcavities at the macrolevel [3]. Much attention has been given to one-dimensional problems in both theoretical and experimental studies. Numerical modeling of the "simplest" (one-dimensional and quasi-one-dimensional) experiments makes it possible for a more detailed analysis of wave patterns in bodies and establishment of the adequacy and limits of applicability of the defining relationships. Moreover, numerical realization of models of such experiments does not require solution of complex boundary problems, thus reducing to a minimum errors introduced by the numerical method of problem solution itself. Carrying out such calculations and comparing the results to experiment allows evaluation of the model chosen for the physical process in the purest possible way.

The concept of mechanics of a degraded medium was used in [4] to develop a model of failure of solid bodies under dynamic loading. In the present study that model will be used for numerical analysis of spallation failure of copper plates in planar rarefaction waves, and the results will be compared to the experiments of [5].

1. To describe material behavior in the process of nonisothermal elastoplastic deformation and damage accumulation the equations of [6] will be used, in which the radius of the yield surface depends on the level of accumulated damage. It will be assumed that the deformation tensor includes elastic deformations which are independent of the loading history and define the final state of the process, plastic deformations which depend on the loading process, and destruction deformations caused by failure of the material as a result of damage accumulation, i.e.,

$$\varepsilon_{ij} = \varepsilon_{ij}^e + \varepsilon_{ij}^p + \varepsilon_{ij}^d, \tag{1.1}$$

where ε_{ij}^e, ε_{ij}^p, ε_{ij}^d are elastic, plastic, and destruction components of ε_{ij}, respectively ($\varepsilon_{ii}^p = 0$, $\varepsilon_{ij}^d = \varepsilon_m^d \delta_{ij}$, $\varepsilon_m^d = \varepsilon_{ii}/3$, i, j = 1, 2, 3).

Upon change in stresses the elastic deformations obey a generalized Hooke's law, and with change in temperature follow the temperature expansion law

$$\dot{e}_{ij}^e = \frac{1}{2G}\dot{S}_{ij} - \frac{\dot{G}}{G}e_{ij}^e; \quad \dot{\varepsilon}_m^e = \frac{1}{3K}\dot{\sigma}_m - \frac{\dot{K}}{K}(\varepsilon_m^e - \alpha T) + \alpha\dot{T} + \dot{\alpha}T. \tag{1.2}$$

Here K = K(T) and G = G(T) are functions of temperature T; $S_{ij} = \sigma_{ij} - \sigma_m\delta_{ij}$ are deviator, and $\sigma_m = \sigma_{ii}/3$, spherical components of the stress tensor σ_{ij}; $e_{ij} = \varepsilon_{ij} - \varepsilon_m\delta_{ij}$ is the small deformation tensor deviator; $\varepsilon_m = \varepsilon_{ii}/3$ is the volume deformation of the medium; K is the volume compression modulus; G is the shear modulus; and α is the linear thermal expansion coefficient of the material matrix.

We write the equation of the yield surface in the Mises form:

$$(S_{ij} - \rho_{ij})(S_{ij} - \rho_{ij}) = (1 - V_v)^{2n}R_p^2. \tag{1.3}$$

Nizhni Novgorod. Translated from Prikladnaya Mekhanika i Tekhnicheskaya Fizika, No. 2, pp. 19-24, March-April, 1993. Original article submitted December 12, 1990; revision submitted February 12, 1992.

0021-8944/93/3402-0169$12.50

According to the associated flow law, we have

$$\dot{e}_{ij}^{p} = \lambda (S_{ij} - \rho_{ij}), \tag{1.4}$$

where λ is a proportionality coefficient determined from the condition of passage of the instantaneous yield surface through the tip of the load vector; $R_p = R_p^0 + \int_0^t q\dot{T}dt$ is the current radius of the yield surface; $\rho_{ij} = \rho_{ij}^0 + \int_0^t g\dot{e}_{ij}^p dt$ are the coordinates of its center; g and q are experimentally determined parameters [6].

The rate of change of the destructive deformation component is related to the rate of change of the relative volume of cavities by the expression [2]

$$\dot{\varepsilon}_m^d = (1/3)\dot{V}_v/(1 - V_v). \tag{1.5}$$

We write the evolution equation for the degradation in the form

$$\dot{V}_v = \begin{cases} -\dfrac{F(V_v)}{\eta}\Delta p_s \operatorname{sign}(p_s), & \Delta p_s > 0, \\ 0, & \Delta p_s \leqslant 0. \end{cases} \tag{1.6}$$

Here

$$F(V_v) = \begin{cases} V_v^{1/3}(1 - V_v)^{2/3}, & V_v \leqslant 1/3, \\ \dfrac{\sqrt[3]{16}}{9} V_v^{-1/3}(1 - V_v)^{-2/3}, & V_v > \dfrac{1}{3}, \end{cases} \quad \Delta p_s = \begin{cases} |p_s| - p_0, & p_s \leqslant 0, \\ |p_s| - \dfrac{p_0}{(1 - V_v)^n}, & p_s > 0; \end{cases}$$

$$p_s = K(1/V_s - 1) + 3K\alpha(T - T_0);$$

V_s is the relative volume of the material matrix; p_s is the pressure in the solid component of the material; $T - T_0$ is the temperature change from T_0 to T; p_0, η, n are parameters of the model.

Reduction in strength of the material due to appearance of microdefects is considered by introducing effective moduli of elasticity [4]:

$$S_{ij} = 2\overline{G}(e_{ij} - e_{ij}^p), \quad e_{ij}^p = \int_0^t \dot{e}_{ij}^p dt,$$

$$\sigma_m = 3\overline{K}\left[\varepsilon_m - \alpha(T - T_0) - \varepsilon_m^d\right], \quad \varepsilon_m^d = \int_0^t \dot{\varepsilon}_m^d dt.$$

where $\overline{G} = G(1 - V_v)\left(1 - \dfrac{6K + 12G}{9K + 8G} V_v\right)$; $\overline{K} = 4GK(1 - V_v)/(4G + 3KV_v)$.

With consideration of degradation we write the material strength criterion in the form

$$J_{2\sigma} - \frac{1}{3}J_{1\sigma}^2 - \frac{\sigma_*}{2}(1 - V_v)^n\left[1 - 3\left(\frac{\tau_*}{\sigma_*}\right)^2\right]J_{1\sigma} \geqslant \frac{1}{2}(1 - V_v)^{2n}\tau_*^2 \tag{1.7}$$

($J_{1\sigma}$ is the first, $J_{2\sigma}$, the second invariant of the stress tensor; and σ_*, τ_* are the strength limits of the material for tension and shear).

Equations of state (1.1)-(1.5) together with the equation of cavity kinetics (1.6) and the failure criterion (1.7) describe the processes of nonisothermal elastoplastic deformation and damage accumulation up to the stage of macrocrack formation.

2. In [5] the problem of collision at a velocity of 185 m/sec of type OFHC copper plates 0.2 and 0.9 cm thick was solved. An oscillogram of the velocity of the target-free surface was presented. A model was proposed to describe spallation in which failure was represented as a process of formation, growth, and merger of micropores.

Below we will present a numerical analysis of this problem, obtained using the expressions presented above. To integrate the system we use an explicit finite difference scheme in Lagrangian variables, introducing an artificial viscosity in shock compression regions [7].

The calculations were preceded by an analysis of the effect of the finite difference scheme parameters (spatial and time steps) upon the results. The step values were selected such that their effect on the results obtained was minimal. A grid with spatial step Δx = 0.01 cm and time step Δt = 0.008 μsec was used. The kinetic parameters of the model of [4]

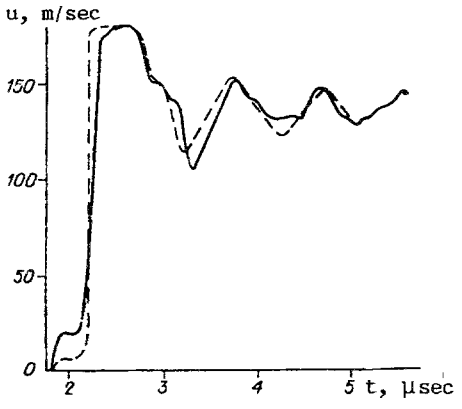

Fig. 1

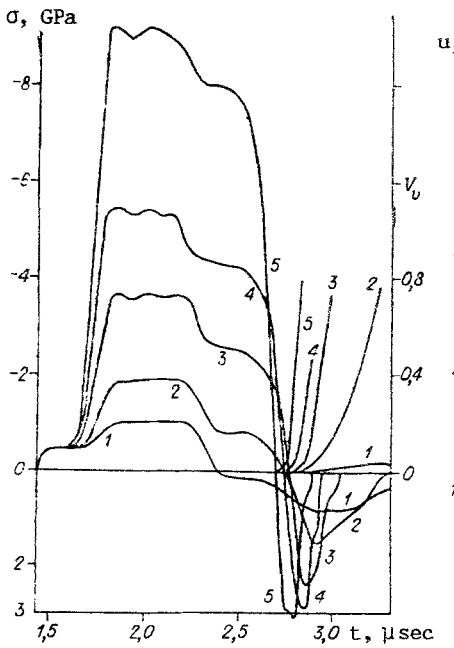

Fig. 2

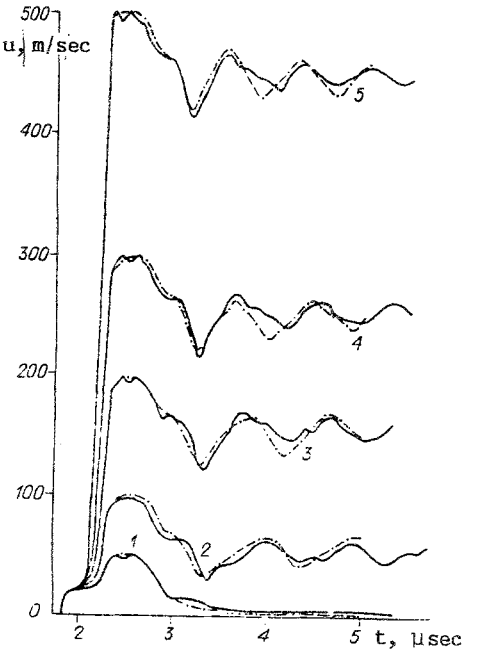

Fig. 3

were determined by comparing experimental data with the calculations. The comparison was based on the principle that the model used should describe the history of the target-free surface velocity, since that history contains information on the kinetics of the failure process and the stresses acting therein.

In Fig. 1 the abscissa represents time, and the ordinate the velocity of motion of the target rear surface (the solid line represents the numerical results of the present study, the dashes, the experimental data of [5]). The good agreement of experiment and theory is evident. These and following calculations were obtained using the following data for copper: density $\rho = 8.92$ g/cm^3, shear modulus $G = 48.4$ GPa; volume compression modulus $K = 136.4$ GPa; yield strength $\sigma_s = 0.2$ GPa; hardening modulus $g = 0.9$ GPa, with kinetic parameters of the model of [4] as follows: $p_0 = 0.5$ GPa, $\eta = 40$ Pa·sec, $n = 0.5$, $\sigma_* = 12$ GPa, $\tau_* = 10$ GPa.

In order to study model sensitivity to change in the collision velocity, and also to verify the accuracy of kinetic parameter determination, a series of calculations were performed for interaction of 0.2 and 0.9 cm thick copper plates at various collision velocities.

Collision conditions and calculation results are presented in Figs. 2, 3, and Table 1, where u_0 is the velocity of the striker plate, σ_- is the calculated maximum value of compressive stresses in the target, σ_+ is the amplitude of the tensile stress in the spallation plane, u_1 is the calculated maximum velocity of the target-free surface, u_2 and u_3 are the velocities at the first minimum and second maximum, respectively, R is the degree of degradation, defined in [8], σ_f is the value of the failure stress [9].

Figure 2 shows the change over time of stress and relative cavity volume in the spallation plane, while Fig. 3 shows the velocity of the target-free surface for various collision velocities. The solid lines of Fig. 3 are calculation results obtained herein, while the dashes are numerical results of [5]. Curve numbering in Figs. 2, 3 corresponds to the variants listed in Table 1.

Upon interaction of the striker and target compression waves move in both directions from the contact boundary, with amplitude determined by the collision velocity. Reflecting from the free surface in the form of oppositely directed unloading waves, they created a region within the target subject to tensile stress. When the pressure reaches a threshold value p_0 the process of damage accumulation begins. With growth in damage density a spallation impulse propagates in both directions from the failure zone.

It is evident from Fig. 2 that the rate of increase of relative cavity volume increases with intensity of the interaction. For a collision with $u_0 = 50$ m/sec only insignificant micro-discontinuities are formed ($V_V = 0.0381$), the appearance of which has practically no effect on the stress-deformed state. When a macrocrack is formed in the target (curves 2-5, Figs. 2, 3), two distinct segments can be distinguished in the curve of relative pore volume

TABLE 1

Variant	u_0, m/sec	σ_-	σ_+	u_1	u_2	u_3	R	σ_f, GPa
		GPa		m/sec				
1	50	0,95	0,80	48	5,5	—	0,115	—
2	100	1,85	1,55	96	29	61	0,635	1,20
3	200	3,65	2,40	197	121	167	0.844	1,36
4	300	5,47	2,91	298	215	266	0,899	1,48
5	500	9,17	3,05	500	415	466	0,932	1,52

vs time, on the first of which ($V_V \leq 0.3$) the growth rate is lower than on the second (when V_V reaches a value of the order of magnitude of 0.3 the merger process begins — breakage of the remaining continuous intervals between pores, which leads to an abrupt increase in the rate of growth of their relative volume). It then develops that the amplitude of tensile stresses in the failure plane increases much more slowly than the amplitude of the compression pulse. Thus, for change in collision velocity from 50 to 500 m/sec the value of σ_+ increases from 0.8 to 3.05 GPa, while σ_- increases from 0.95 to 9.17 GPa. This is apparently due to the effect of the growing microdefects on the character of material deformation.

Determining the thickness of the spallation lamina is of importance in studying the failure processes. It should be noted that pores develop in a large number of elements of the finite difference grid, althrough their highest concentration ($V_V > 0.3$) occurs in a quite narrow zone ($0.67 \leq x \leq 0.71$ cm), which is where merger of micropores and formation of the spallation surface occur. Thus, the position of the main crack in variants 2-5 coincides with the data of [5] with good accuracy.

The failure stress value [9] and the degree of material damage [8] are often found by direct processing of the target-free surface velocity.

The critical stress value is given by the expression

$$\sigma_f = 0{,}5\rho c(u_1 - u_2) \tag{2.1}$$

(where c is the velocity of elastic longitudinal wave propagation).

Results of σ_f calculations with Eq. (2.1) are given in Table 1. It is evident that the σ_f value depends on collision velocity (increasing with increase in collision velocity), while its lower limit $\sigma_f = 1.2$ GPa coincides with results of spallation strength measurements in OFHC copper [10]. Although this dependence weakens with further increase in collision velocity (for a change in collision velocity from 100 to 300 m/sec the value of σ_f increases from 1.20 to 1.48 GPa, while for an increase in velocity from 300 to 500 m/sec it increases only from 1.48 to 1.52 GPa) it is clear that Eq. (2.1) must be used with caution.

To estimate the degree of material damage [8] proposed the parameter

$$R = u_3/u_1, \quad 0 < R < 1 \tag{2.2}$$

is used.

It was noted in [8] that R = 0.5 corresponds to incipient spallation. It is evident (see Table 1) that with increase in collision velocity the value of R increases. Comparison of R to the relative cavity volume V_V (Fig. 2) shows that correlation occurs only up to a certain limit (before formation of a macrocrack in the material). This can apparently be explained by the fact that, depending on collision conditions and the physicomechanical properties of the bodies considered, formation of a spallation surface may occur at different degrees of damage [2]. Thus, according to the data of [11], the damage level at which formation of macrocracks occurs can vary over the range 0.2 to 0.8.

LITERATURE CITED

1. Ya. B. Zel'dovich and Yu. P. Raizer, Physics of Shock Waves and High Temperature Hydrodynamic Phenomena [in Russian], Nauka, Moscow (1966).
2. N. Kh. Akhmadeev, Dynamic Failure of Solids in Stress Waves [in Russian], Akad. Nauk SSSR, Ufa (1988).
3. D. R. Kurran, L. Simén, and D. A. Shoki, "Microstructure and failure dynamics," in: Shock Waves and High Speed Metal Deformation Phenomena [in Russian], Metallurgiya, Moscow (1984).

4. I. A. Volkov, "Mathematical modeling of damage accumulation in dynamic deformation of material," in: Practical Problems in Strength and Plasticity. Solution Methods: All-Union Inter-VUZ Collection [in Russian], Nizhnii Novgorod, Nizh. Novg. Univ. (1991).
5. A. M. Rajendran, M. A. Dietenberger, and D. J. Growe, "A void-growth based failure model to describe spallation," J. Appl. Phys., 65, No. 4 (1989).
6. Yu. G. Korotkikh and A. G. Ugodchikov, Equations of State for Low-Cycle Loading [in Russian], Nauka, Moscow (1981).
7. M. L. Wilkins, "Elastoplastic flow calculation," in: Computation Methods in Hydrodynamics [Russian translation], Mir, Moscow (1967).
8. S. Cochran and D. Banner, "Spall studies in uranium," J. Appl. Phys., 48, No. 7 (1977).
9. G. V. Stepanov, Elastoplastic Deformation and Failure of Materials under Impulsive Loading [in Russian], Naukova Dumka, Kiev (1991).
10. G. I. Kanel' and V. E. Fortov, "Mechanical properties of condensed media under intense impulsive loads," Usp. Mekh., 10, No. 3 (1987).
11. J. Lemetre, "A continuum model of degradations, used to calculate failure of plastic materials," Tr. ASME, 107, No. 1 (1985).

PROPAGATION OF SHOCK WAVES IN POLYDISPERSE GAS SUSPENSIONS

A. G. Kutushev and S. P. Rodionov

UDC 532.529:518.5

Actual gas suspensions are always polydisperse, i.e., they contain particles of different sizes. The presence of only one or a few particle fractions, each of which contains particles of the same size, is presumed for the description of particle motion in most of the presently known models of gas suspensions [1-4]. The drawback of such a description is that the actual continuous size distribution of the particles is ignored. The equations of motion of polydisperse gas suspensions with a continuous particle size distribution function have been considered in a linear (acoustic) approximation in [5, 6]. It was shown in [6] that the motion of a polydisperse gas suspension cannot be described completely, in general, using a model of a monodisperse gas suspension. The problem of describing the motion of a polydisperse gas suspension with a continuous particle size distribution function behind nonlinear (shock) waves arises in this connection.

In the present paper we obtain a system of integrodifferential equations of motion of an inert, polydisperse gas suspension with a continuous particle size distribution function with allowance for collisions between particles of different sizes. On the basis of the equations derived and the method developed for their numerical solution, we calculate the structure and damping of shocks in polydisperse gas suspensions. We establish the satisfactory agreement between the calculated data and the results of [7, 8]. We show that the structure of shocks in polydisperse gas suspensions depends to a considerable extent on the disperse composition of the ensemble of particles.

1. Basic Equations. By analogy with [5, 6], a polydisperse gas suspension is assumed to consist of a collection of an infinite number of monodisperse fractions of spherical incompressible particles, the radius of which is in the interval from a to a + da. The number of particles in one such fraction per unit volume is

$$d\tilde{n} = \tilde{N}(a, x, t)\,da,$$

where x is the spatial coordinate of the particles; t is time; $\tilde{N}$ is the size distribution function of the particles. The total number of particles of all sizes per unit volume of the mixture is

$$n = \int_{a_{\min}}^{a_{\max}} \tilde{N}(a, x, t)\,da$$

Tyumen'. Translated from Prikladnaya Mekhanika i Tekhnicheskaya Fizika, No. 2, pp. 24-31, March-April, 1993. Original article submitted July 23, 1991; revision submitted January 29, 1992.